Coupling Between Neuronal Firing, Field Potentials, and fMRI in Human Auditory Cortex

Roy Mukamel *et al.*

Science **309**, 951 (2005);
DOI: 10.1126/science.1110913

nized groups of neurons oscillate (*15*, *22*) and reaches a maximum when cells engage in high-frequency gamma oscillations.

How do changes in the temporal patterning of responses influence hemodynamic responses? There is evidence that synchronization in the gamma frequency range is associated with oscillatory, tightly synchronized discharges of inhibitory interneurons (*23*) leading to periodic inhibition of pyramidal cells. These inhibitory postsynaptic potentials, in turn, synchronize pyramidal cells by confining their discharges to the depolarizing peaks of the membrane potential oscillations (*24*). Thus, when cortical networks engage in gamma oscillations, inhibitory interneurons are highly active, and as their discharges are phase-locked to the oscillations (*23*), their activity increases with oscillation frequency. Therefore, we propose that the hemodynamic responses associated with gamma oscillations are mainly initiated by the firing of inhibitory interneurons.

Although inhibitory interneurons constitute only about 20% of the cortical neurons, it is likely that they substantially contribute to local energy consumption. They fire at very high frequencies and distribute their numerous synapses exclusively within adjacent cortical volumes. The hypothesis that interneuron activity is a major cause of the hemodynamic response (*25*) is well compatible with the fact that interneurons contain enzymes for the synthesis of vasoactive compounds such as NO and vasoactive peptides (*26*, *27*). In this cascade, the elevated calcium concentration is suggested to play a major role (*25*).

This interpretation resolves some of the discrepancies between BOLD studies and unit recordings. Deficits in visual processing in amblyopia are well reflected by evoked potentials and hemodynamic responses, although they are undetectable in discharge rates (*7*). Attentional shifts in the absence of sensory stimulation (*28*) and mental imagery (*29*) are associated with BOLD responses, and these cognitive processes are associated with increased oscillatory activity in the gamma frequency band (*14*, *30*). Other cognitive and executive functions such as figure-ground segmentation, expectancy, sensory-motor coordination, short-term memory, and movement preparation are associated with enhanced oscillatory activity in the beta and gamma frequency range (*31*, *32*). Hemodynamic responses may thus be ideally suited to visualize neural processes associated with higher cognitive and executive functions.

References and Notes

1. R. D. Frostig, E. E. Lieke, D. Y. Ts'o, A. Grinvald, *Proc. Natl. Acad. Sci. U.S.A.* **87**, 6082 (1990).
2. S. Ogawa, T. M. Lee, A. R. Kay, D. W. Tank, *Proc. Natl. Acad. Sci. U.S.A.* **87**, 9868 (1990).
3. G. Rees, K. Friston, C. Koch, *Nat. Neurosci.* **3**, 716 (2000).
4. A. J. Smith *et al.*, *Proc. Natl. Acad. Sci. U.S.A.* **99**, 10765 (2002).
5. O. J. Arthurs, E. J. Williams, T. A. Carpenter, J. D. Pickard, S. J. Boniface, *Neuroscience* **101**, 803 (2000).
6. S. Sheth *et al.*, *Neuroimage* **19**, 884 (2003).
7. K. E. Schmidt, W. Singer, R. A. Galuske, *J. Neurophysiol.* **91**, 1661 (2004).
8. U. Mitzdorf, W. Singer, *Exp. Brain Res.* **33**, 371 (1978).
9. N. K. Logothetis, J. Pauls, M. Augath, T. Trinath, A. Oeltermann, *Nature* **412**, 150 (2001).
10. C. Kayser, M. Kim, K. Ugurbil, D. S. Kim, P. Konig, *Cereb. Cortex.* **14**, 881 (2004).
11. C. Mathiesen, K. Caesar, N. Akgoren, M. Lauritzen, *J. Physiol.* **512**, 555 (1998).
12. D. A. McCormick, T. Bal, *Annu. Rev. Neurosci.* **20**, 185 (1997).
13. M. Steriade, *Science* **272**, 225 (1996).
14. P. Fries, J. H. Reynolds, A. E. Rorie, R. Desimone, *Science* **291**, 1560 (2001).
15. S. Herculano-Houzel, M. H. Munk, S. Neuenschwander, W. Singer, *J. Neurosci.* **19**, 3992 (1999).
16. R. Rodriguez, U. Kallenbach, W. Singer, M. H. Munk, *J. Neurosci.* **24**, 10369 (2004).
17. Materials and methods are available as supporting material on *Science* Online.
18. G. M. Boynton, S. A. Engel, G. H. Glover, D. J. Heeger, *J. Neurosci.* **16**, 4207 (1996).
19. O. J. Arthurs, S. Boniface, *Trends Neurosci.* **25**, 27 (2002).
20. N. Pouratian *et al.*, *Magn. Reson. Med.* **47**, 766 (2002).
21. D. Attwell, S. B. Laughlin, *J. Cereb. Blood Flow Metab.* **21**, 1133 (2001).
22. M. Volgushev, M. Chistiakova, W. Singer, *Neuroscience* **83**, 15 (1998).
23. R. D. Traub, M. A. Whittington, I. M. Stanford, J. G. Jefferys, *Nature* **383**, 621 (1996).
24. R. Azouz, C. M. Gray, *J. Neurosci.* **19**, 2209 (1999).
25. M. Lauritzen, *Nat. Rev. Neurosci.* **6**, 77 (2005).
26. J. G. Valtschanoff *et al.*, *Neurosci. Lett.* **157**, 157 (1993).
27. B. Cauli *et al.*, *J. Neurosci.* **24**, 8940 (2004).
28. S. Kastner, M. A. Pinsk, P. De Weerd, R. Desimone, L. G. Ungerleider, *Neuron* **22**, 751 (1999).
29. S. M. Kosslyn, G. Ganis, W. L. Thompson, *Nat. Rev. Neurosci.* **2**, 635 (2001).
30. M. M. Muller, T. Gruber, A. Keil, *Int. J. Psychophysiol.* **38**, 283 (2000).
31. C. Tallon-Baudry, *J. Physiol. (Paris)* **97**, 355 (2003).
32. A. K. Engel, P. Fries, W. Singer, *Nat. Rev. Neurosci.* **2**, 704 (2001).

33. We thank H. Klon-Lipok and E. Scheibinger for technical assistance and M. Wibral, M. Lutzenburg, and G. Pipa for helpful comments and suggestions on the project.

Supporting Online Material

www.sciencemag.org/cgi/content/full/309/5736/948/DC1
Materials and Methods
Figs. S1 to S4
References

10 February 2005; accepted 10 June 2005
10.1126/science.1110948

Coupling Between Neuronal Firing, Field Potentials, and fMRI in Human Auditory Cortex

Roy Mukamel,[1] Hagar Gelbard,[1] Amos Arieli,[1] Uri Hasson,[2] Itzhak Fried,[3,4]* Rafael Malach[1]*

Functional magnetic resonance imaging (fMRI) is an important tool for investigating human brain function, but the relationship between the hemodynamically based fMRI signals in the human brain and the underlying neuronal activity is unclear. We recorded single unit activity and local field potentials in auditory cortex of two neurosurgical patients and compared them with the fMRI signals of 11 healthy subjects during presentation of an identical movie segment. The predicted fMRI signals derived from single units and the measured fMRI signals from auditory cortex showed a highly significant correlation ($r = 0.75$, $P < 10^{-47}$). Thus, fMRI signals can provide a reliable measure of the firing rate of human cortical neurons.

A major concern in the rapidly expanding field of functional magnetic resonance imaging (fMRI) has been the absence of a quantitative relationship between blood oxygenated level–dependent (BOLD) fMRI signals and neuronal activity. Several studies have attempted to characterize this relationship (*1*–*10*). In anesthetized monkeys, a higher correlation of the fMRI signal to the local field potential (LFP) was found compared with spike activity (*11*). However, the implications of these studies to the awake, conscious human brain are unclear.

Recently, we reported that movie stimuli are particularly effective in producing a widespread and robust correlation in the evoked fMRI signals across different subjects (*12*). Here, we used this phenomenon of intersubject correlation to examine the nature of the coupling between fMRI signals and neuronal activity in the sensory cortex of alert humans.

We recorded from 53 single neurons in Heschl's gyrus (auditory cortex) of two native English-speaking patients with epilepsy monitored with intracranial depth electrodes for potential surgical treatment (*13*). Recordings were done while the patients saw two repetitions of a 9-min segment from a popular

[1]Department of Neurobiology, Weizmann Institute of Science, Rehovot 76100, Israel. [2]Center for Neural Science, New York University, New York, NY 10003, USA. [3]Division of Neurosurgery, David Geffen School of Medicine, and Semel Institute for Neuroscience and Human Behavior, University of California Los Angeles (UCLA), Los Angeles, CA 90095, USA. [4]Functional Neurosurgery Unit, Tel Aviv Medical Center and Sackler School of Medicine, Tel Aviv University, Tel Aviv 69978, Israel.

*To whom correspondence should be addressed. E-mail: rafi.malach@weizmann.ac.il (R.M.); ifried@mednet.ucla.edu (I.F.)

English-speaking movie. Twenty out of 30 neurons in patient 1 and 17 out of 23 in patient 2 showed reproducible auditory responses. The spiking activity of these neurons in each patient was summed and converted into a predicted fMRI BOLD response (spike predictor) by convolution with a standard hemodynamic response function (gamma function) (*2*, *14*) (Fig. 1). In parallel, we performed fMRI scans on 11 healthy subjects while they watched the same movie segment (*13*). All subjects spoke English as a second language. We then used the spike predictor of each patient (e.g., Fig. 1C for patient 1) as a regressor in a conventional general linear model (GLM) analysis of the fMRI signals obtained from the healthy subjects. Figure 2 shows the multiparticipant average activation map of 11 subjects as derived from the spike predictor of patient 1, projected onto the reconstructed folded hemispheres of the patient. The map has its basis in the average of all single-subject data, transformed into common Talairach space (*15*). On the basis of postoperative computer tomography scans, we could estimate the location of the recording electrode ("e" in Fig. 2). The most significant activation foci were localized to Heschl's gyrus in close proximity to the electrode's location. Significant activation in the same region was also found in individual subjects (see individual maps in fig. S1). In the second patient, the data followed a similar trend (fig. S2). No significant activation was revealed with the use of a predictor derived from the soundwave amplitude (*13*). Furthermore, control fMRI data, recorded while subjects viewed the same movie segment with no sound or viewed a different movie segment, revealed no correlation with the spike predictor (fig. S3).

We sampled the fMRI time course in Heschl's gyrus of each subject by using the spike predictors of the patients. To ensure statistical independence of region of interest (ROI) definition and sampling of signal time course, we used the internal localizer design in which nonoverlapping time segments of the spike predictor were used for ROI definition and for sampling (*13*, *16*). Time courses were then averaged across subjects. The average fMRI time courses are shown in the bottom graphs of Fig. 3 and in fig. S4. These time courses are superimposed on the spike predictor (black trace). The correlation coefficients between the averaged fMRI signal and the spike predictors were 0.75 ($P < 10^{-47}$) for patient 1 and 0.56 ($P < 10^{-28}$) for patient 2. The sampled fMRI signals were slightly different for the two patients, because their

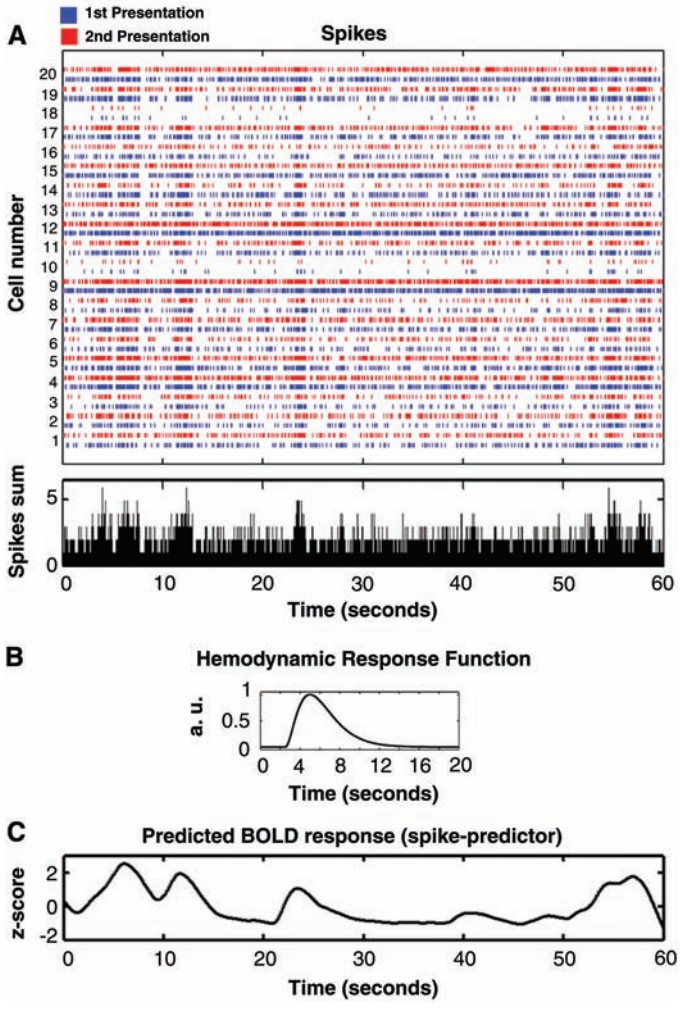

Fig. 1. The fMRI BOLD predictor created from spikes of patient 1. (**A**) Raster display of spike trains from all 20 cells during the first (blue) and second (red) movie presentation. The black histogram displays the population summed activity. The summed activity was convolved with a gamma hemodynamic response function (**B**). The resulting time course was *Z*-score normalized (**C**) and used as a predictor for the BOLD fMRI signal. a.u., arbitrary units.

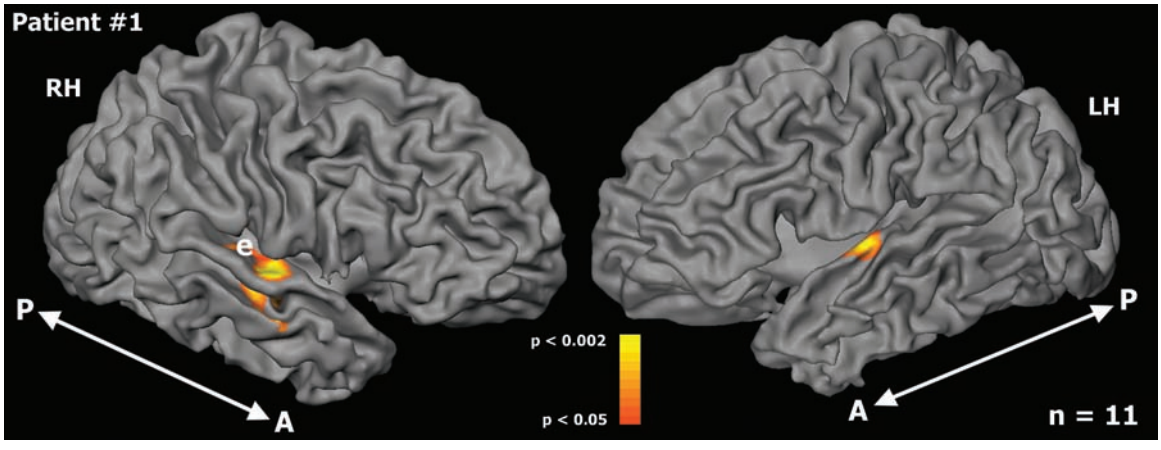

Fig. 2. The fMRI BOLD activation map derived from the spike predictor. Multisubject map ($n = 11$) obtained with use of the spike predictor of patient 1. The fMRI activations are shown on the reconstructed folded hemispheres of the patient. Activations were obtained with a random effect multi-GLM test by using the predictor obtained from the average spike train (20 cells) of patient 1. Note the localized activations in Heschl's gyrus corresponding to the site of spike recordings in the patient (denoted by "e"). RH and LH, right and left hemisphere, respectively; A, anterior; P, posterior.

spike predictors defined slightly different ROIs, possibly due to the fact that the electrode position in the two patients was not identical [for exact Talairach coordinates see (*13*)].

The amount of correlation between the fMRI signals and spike predictors modulated along the 9-min movie timeline. For example, during stretches of silence in the movie there was no stimulus-evoked activity in auditory cortex, and no correlation is expected between the spontaneous neural activity in different individuals. In order to isolate times of high correlation between different individuals, we calculated a moving correlation function between the fMRI signals of the healthy subjects (green traces in Fig. 3) (*13*). Periods of high intersubject correlation (light gray shaded regions) largely coincided with periods of high correlation between the BOLD fMRI signal and the spike predictors. Thus, although the correlations between the neuronal and fMRI signals were 0.75 and 0.56 for the two patients for the entire duration of the recording, these correlations climbed to 0.9 ($P < 10^{-30}$) and 0.72 ($P < 10^{-19}$) when only 30% of the time course, showing the highest interparticipant correlations, was considered.

The electrophysiological recordings from the two patients were continuous, spanning 1 to 14 kHz, allowing us to examine also the relationship between the LFPs and the fMRI signals. LFPs are typically of lower frequencies (~1 to 130 Hz) and likely relate to dendritic synaptic activity (*1*). We created fMRI predicted signals from the power modulations of the LFP signals at different frequencies (LFP predictors) (*13*). Figure 4A depicts the correlation between the different LFP predictors (corresponding to different frequency bands) and the spike predictor (cyan) and also their correlation with the average fMRI signal sampled with the spike predictor (orange) for patient 1. Interestingly, at different frequency bands there was a clear inversion of the correlation value between the fMRI data and the LFP signal from negative correlation at low LFP frequencies (5 to 15 Hz, green) to strong positive correlation at high frequencies (40 to 130 Hz, yellow). Also there was a strong correlation between the spike predictor and LFP predictor at high frequencies (cyan trace). We generated LFP predictors for the two frequency bands (5 to 15 Hz and 40 to 130 Hz) (*13*). All three predictors (spikes and low- and high-frequency LFPs) were most significantly correlated with the fMRI signal in Heschl's gyrus (with a sign inversion for the low frequency LFP predictor) (Fig. 4, B to D).

Correlation values of high-frequency LFP and spike predictors with fMRI BOLD signal of each subject were compared. The results show similar correlations derived from these two predictors: for patient 1, spike predictor correlation of 0.5 ± 0.04 SEM and LFP predictor of 0.46 ± 0.04; for patient 2, spike predictor correlation of 0.39 ± 0.04 SEM and LFP predictor correlation of 0.39 ± 0.04. Thus, in patient 1, the correlation with BOLD was slightly better for the spike predictor than the high-frequency LFP-predictor ($P < 0.05$, paired t test), whereas no significant difference was found in patient 2 ($P < 0.48$, paired t test). For spike and LFP predictors, their corresponding fMRI signals, and spectral analysis of stimulus soundwave, see fig. S5.

Lastly, although the measured time courses were rather short, the availability of both spiking activity and fMRI responses to the same stimulus allowed us to obtain a data-driven, objective estimate of the human hemodynamic response function, coupling the spikes and fMRI BOLD signal. By using standard deconvolution methods (*13*), we obtained such functions for the two fMRI data sets, sampled at a rate of 1 and 1/3 Hz (orange and purple traces in fig. S6). The obtained functions were quite compatible with the current estimates of the BOLD hemodynamic response function (black trace) (*2*, *14*). Noticeably, the data sampled at the faster rate exhibited a small but significant ($P < 10^{-4}$) initial decrease in the BOLD signal of four out of six subjects (fig. S6, gray circles) (*13*, *17*, *18*).

Our results indicate a high linear correlation between spiking activity, high-frequency LFP, and fMRI BOLD signal measured in human auditory cortex during natural stimulation. We cannot rule out the possibility that under different physiological conditions or in different brain regions there may be a decoupling between spiking activity and the BOLD signal (*11*). Because in our stimulation paradigm the spiking activity was highly correlated with the high-frequency LFP (cyan trace, Fig. 4A), our results cannot identify one or the other as the driving source behind the BOLD signal (*9*–*11*, *19*, *20*). However, regardless of the mechanism underlying the BOLD signal, the broad methodological implication of our findings lies in the demonstration that, at least under natural stimulus conditions, BOLD fMRI signals can be trusted as a faithful measure of the average firing rate of the underlying population.

The high correlation found does not necessarily imply lack of variability in the fMRI

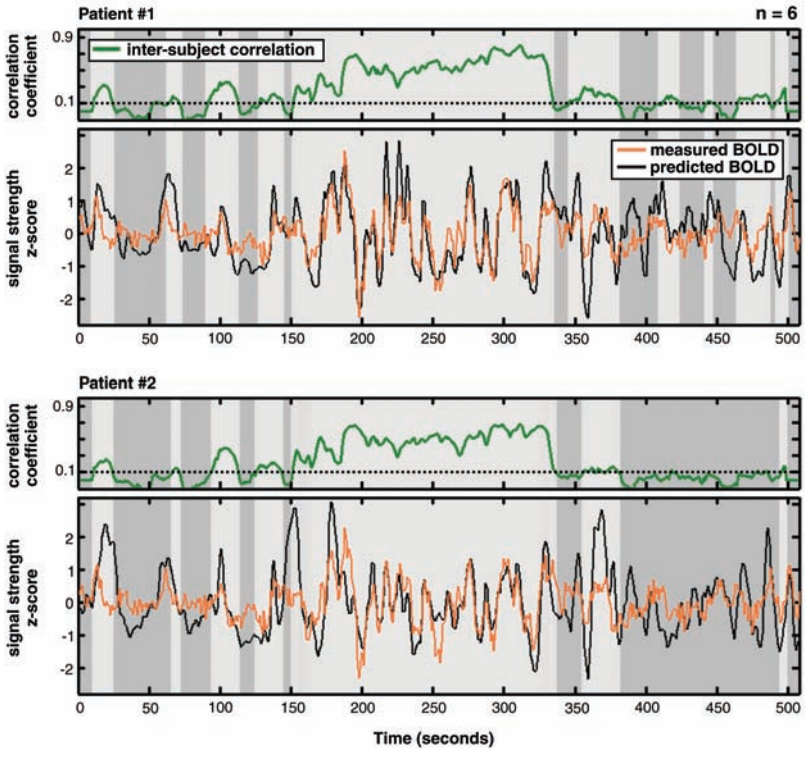

Fig. 3. Correlation of the spike predictor with measured fMRI activation. fMRI BOLD activations in Heschl's gyrus of each of the six subjects were sampled by using the spike predictor of each patient (top, patient 1; bottom, patient 2). Bottom graphs depict the average measured BOLD activation of all six subjects (orange traces) together with the predicted BOLD created from the average spike train of each patient (black traces). The overall correlations between the average BOLD signal and the spike predictors were 0.73 for patient 1 and 0.55 for patient 2. Top graphs depict the average intersubject correlation (green traces) between BOLD activations of all subject pairs calculated in sliding windows of 21 s (*13*). Light gray regions correspond to times in which the average intersubject correlation was greater than 0.1, whereas dark gray regions correspond to times in which the average intersubject correlation was smaller than 0.1. The correlation between the BOLD signal and spike predictors increased at high (> 0.1) levels of intersubject correlations to 0.81 (0.6) (light gray regions) and further increased to 0.9 (0.72) in the top 30% epochs.

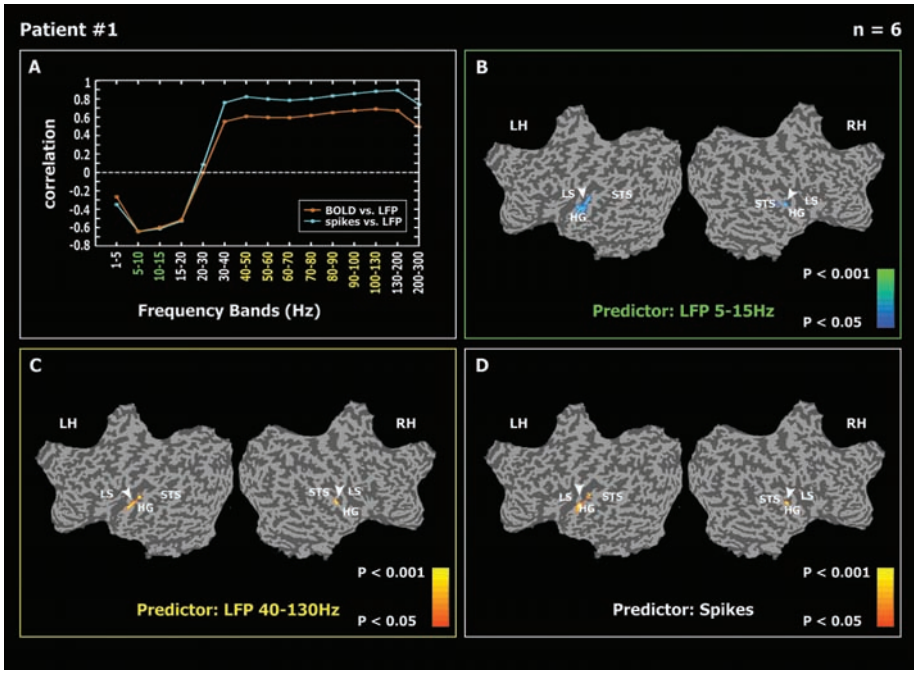

Fig. 4. Correlation maps between fMRI BOLD signal and different components of the electrophysiological measurements. (**A**) The correlation of the different LFP predictors of patient 1 (*13*) with the average fMRI BOLD signal in Heschl's gyrus (orange trace) and with the spike predictor (cyan trace) as a function of frequency band. Note the strong negative correlations between the BOLD activation and the low-frequency LFPs (5 to 15 Hz) and the strong positive correlation with the high-frequency LFPs (40 to 130 Hz). (B to D) The multisubject random-effect GLM map correlating the BOLD signal of six participants with the low-frequency (5 to 15Hz) LFP predictor (**B**), the high-frequency (40 to 130 Hz) LFP predictor (**C**), and the spike predictor (**D**). LS, lateral sulcus; STS, superior temporal sulcus; HG, Heschl's gyrus; RH and LH, right and left hemisphere, respectively. Arrowheads point to regions of highly significant correlation in Heschl's gyrus.

signals. Note that the spikes-to-BOLD correlation obtained for group-averaged fMRI responses was higher (0.75 for patient 1 and 0.56 for patient 2) than that obtained for individual subjects (0.5 and 0.46, respectively).

A particularly important result was the inversion in the coupling of LFP to BOLD, moving from positive correlations at high, gamma-range frequencies (40 to 130 Hz) (*21*) to negative correlations at the low, alpha-range frequencies (5 to 15 Hz) (*22*, *23*). This result is compatible with the notion that electroencephalogram signals in the alpha band frequencies are diminished in times of high cognitive processing and that sensory stimulation leads to desynchronization of slow potentials (*24*).

The fact that the correlation between the spikes, high-frequency LFPs, and fMRI signal in Heschl's gyrus was high despite the extremely noisy MRI environment indicates that human auditory representations at the cortex level deemphasize low-level auditory signals such as loud beeps (*25*, *26*). This is also illustrated in the relatively low (albeit still significant) fMRI responses to high sound-amplitude events (e.g., gunshots and explosions) during the movie compared with speech events (fig. S4) and the weak correlation of the activations with the sound-wave amplitude (figs. S3 and S5).

Our results also have implications for human sensory representations during natural stimulation. The single-unit signal was derived from a small population (~20) of active neurons, whereas the fMRI signals reflect the population activity of millions of neurons (*8*). The fact that firing rate in a mere ~20 responsive neurons was sufficient to capture such a large fraction of the fMRI signal variance points to a highly distributed profile (*27*) of slow auditory responses. In such a representation, auditory neurons contain a strong element of correlation between neighboring neurons during natural sensory stimulation, because they are all driven, albeit to a varying extent, by multiple auditory events (Fig. 1A).

Several intervening factors could have disrupted the correlation between the electrophysiological and fMRI signals. First, the electrophysiological signals were recorded in a quiet hospital room, whereas the fMRI signals were recorded in a typical, acoustically noisy fMRI setup. Second, the small sample of neurons we recorded was unlikely to precisely represent the averaged response profile of the neuronal populations in the imaged fMRI voxels. Lastly, there were individual differences between the patients and the fMRI subjects. Thus, under optimal conditions, such as recording both signals in the same participant, the real physiological coupling between the neuronal firing rates and fMRI BOLD signals may be even stronger than measured.

References and Notes

1. N. K. Logothetis, B. A. Wandell, *Annu. Rev. Physiol.* **66**, 735 (2004).
2. G. M. Boynton, S. A. Engel, G. H. Glover, D. J. Heeger, *J. Neurosci.* **16**, 4207 (1996).
3. A. M. Dale, R. L. Buckner, *Hum. Brain Mapp.* **5**, 329 (1997).
4. G. K. Aguirre, E. Zarahn, M. D'Esposito, *Neuroimage* **8**, 360 (1998).
5. D. A. Handwerker, J. M. Ollinger, M. D'Esposito, *Neuroimage* **21**, 1639 (2004).
6. D. J. Heeger, A. C. Huk, W. S. Geisler, D. G. Albrecht, *Nat. Neurosci.* **3**, 631 (2000).
7. G. Rees, K. Friston, C. Koch, *Nat. Neurosci.* **3**, 716 (2000).
8. I. Levy, U. Hasson, R. Malach, *Curr. Biol.* **14**, 996 (2004).
9. D. Attwell, C. Iadecola, *Trends Neurosci.* **25**, 621 (2002).
10. C. Iadecola, *Nat. Rev. Neurosci.* **5**, 347 (2004).
11. N. K. Logothetis, J. Pauls, M. Augath, T. Trinath, A. Oeltermann, *Nature* **412**, 150 (2001).
12. U. Hasson, Y. Nir, I. Levy, G. Fuhrmann, R. Malach, *Science* **303**, 1634 (2004).
13. Materials and methods are available as supporting material on *Science* Online.
14. R. Goebel, *Neuroimage* **3**, S604 (1996).
15. J. Talairach, P. Tournoux, *Co-Planar Stereotaxic Atlas of the Human Brain* (Thieme Medical, New York, 1988).
16. Y. Lerner, T. Hendler, R. Malach, *Cereb. Cortex* **12**, 163 (2002).
17. B. M. Ances, *J. Cereb. Blood Flow Metab.* **24**, 1 (2004).
18. E. Yacoub, X. Hu, *Magn. Reson. Med.* **45**, 184 (2001).
19. K. Caesar, K. Thomsen, M. Lauritzen, *Proc. Natl. Acad. Sci. U.S.A.* **100**, 16000 (2003).
20. C. Mathiesen, K. Caesar, N. Akgoren, M. Lauritzen, *J. Physiol.* **512**, 555 (1998).
21. M. Siegel, P. Konig, *J. Neurosci.* **23**, 4251 (2003).
22. M. Moosmann *et al.*, *Neuroimage* **20**, 145 (2003).
23. H. Laufs *et al.*, *Proc. Natl. Acad. Sci. U.S.A.* **100**, 11053 (2003).
24. T. V. Sewards, M. A. Sewards, *Int. J. Psychophysiol.* **32**, 35 (1999).
25. P. Belin, R. J. Zatorre, P. Lafaille, P. Ahad, B. Pike, *Nature* **403**, 309 (2000).
26. A. L. Giraud *et al.*, *J. Neurophysiol.* **84**, 1588 (2000).
27. J. V. Haxby *et al.*, *Science* **293**, 2425 (2001).

28. This study was funded by an Israeli Science Foundation grant to R.M., a U.S.-Israel Binational Science Foundation grant to I.F. and R.M., and a National Institute of Neurological Disorders and Stroke grant to I.F. The authors thank the patients for their cooperation in participating in the study. We also thank Y. Nir for helpful suggestions; M. Harel for help with the fMRI data; D. Malah for help with the deconvolution algorithm; D. Heeger, S. Gilaie-Dotan, and A. Amedi for reading the manuscript; and E. Isham, E. Ho, T. A. Fields, E. Behnke and C. Wilson for technical assistance.

Supporting Online Material

www.sciencemag.org/cgi/content/full/309/5736/951/DC1
Materials and Methods
Figs. S1 to S6

10 February 2005; accepted 10 June 2005
10.1126/science.1110913